JOC Article

Remarkable Features of the McMurry Reaction Conditions in Dimerization of Formyl- and 2-Formylvinylpurpurinimides. Electrochemistry of Monomeric Ni(II) Purpurinimide and the Corresponding Dyads

Lalit N. Goswami,[†] Manivannan Ethirajan,[†] Mahabeer P. Dobhal,[†] Min Zhang,[‡] Joseph R. Missert,[†] Masayuki Shibata,[§] Karl M. Kadish,*[,‡] and Ravindra K. Pandey*[,†]

Chemistry Division, PDT Center, Cell Stress Biology, Roswell Park Cancer Institute, Buffalo, New York 14263, Department of Chemistry, University of Houston, Houston, Texas 77204-5003, and Department of Health Informatics, School of Health Related Professions, University of Medicine and Dentistry of New Jersey, Room 35065, Bergen Street, Newark, New Jersey 07107

ravindra.pandey@roswellpark.org; kkadish@uh.edu

Received September 3, 2008

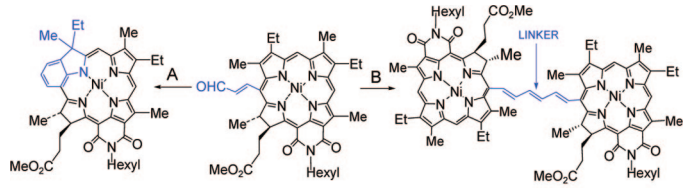

Reagents. A: $TiCl_3(DME)_{1.5}Zn(Cu)$ B: $TiCl_4$ / Zn

To investigate the electrochemical properties of purpurinimide dyads and electron transfer sites for their reduction and oxidation, a series of dimers with variable C−C linkages were synthesized. For the preparation of these novel structures, the formyl and 2-formylvinyl substituents were regioselectively introduced at positions 3 and 20 of Ni(II) purpurinimides by the Vilsmeier reaction. The Ni(II) complexes were then subjected to the McMurry reaction under two different conditions with unexpected results. For example, the reaction of formyl purpurinimides with $TiCl_3(DME)_{1.5}$ failed to produce the desired C−C dimers, and the starting compounds were recovered almost quantitatively. Under similar reaction conditions, the 20-(2-formylvinyl)purpurinimide also did not dimerize but produced instead unexpected benzoisobacteriochlorins via an intramolecular cyclization. However, treatment of the 3-formyl- and 20-formylpurpurinimides with $TiCl_4$/Zn produced corresponding dimers linked with one double bond (*trans*) in modest yields. Under similar conditions, Ni(II) purpurinimides containing a 2-formylvinyl substituent either at position 3 or at position 20 afforded the respective C−C dimers, where the purpurinimide moieties were joined with a *trans-trans-trans* hexatriene linker. Molecular modeling data suggest that the nature of the conformational energy difference found in all *trans* vs *trans-cis-trans* conformers of the dimers connected by a hexatriene linker at the *meso*- or β-position of the macrocycle is not because of the intrinsic conformational energy difference of the linker region, which is identical for both dimers.

Introduction

The McMurry reaction dealing with the use of low-valent titanium complexes has been extensively used for reductive coupling of carbonyls to olefins.[1] It is an exceptionally versatile bond construction method in organic synthesis and in many cases is the best approach for the preparation of highly complex and strained cyclic ring systems.[2] This reaction is usually carried out in two steps: reduction of $TiCl_4$ or $TiCl_3$, followed by addition of the carbonyl substrate. The nature of the titanium reagent as well as the solvent, temperature, and reaction time has a strong influence on eventual formation of the resulting product. Several improved procedures are in the literature for

[†] Roswell Park Cancer Institute.
[‡] University of Houston.
[§] University of Medicine and Dentistry of New Jersey.

(1) McMurry, J. E. *Chem. Rev.* **1989**, *89*, 1513–1524, and references cited therein.

(2) Robertson, G. M. In *Comprehensive Organic Synthesis: Carbon−Carbon Bond Formation*, Trost, B. M., Fleming, I., Heatkcock, C. H., Eds.; Pergmon Press: New York, 1991; Vol. 3, pp 563−611.

10.1021/jo8019237 CCC: $40.75
Published on Web 12/15/2008

the preparation of homodimers, and the recommended "optimized method" is to use a $TiCl_3(DME)_{1.5}$−Zn(Cu) combination.[3]

We were interested in extending this approach to the purpurinimide system for a number of reasons. In our previous studies with a series of porphyrin- and chlorin-fullerene systems, we have shown that the presence of a purpurinimide moiety makes a significant impact in producing long-lived charge-separated states,[4−6] and such a characteristic could be useful in designing improved synthetic models to understand the initial charge separation process in photosynthesis. The purpurinimide system also provides an enormous opportunity to introduce carbonyl substituents at the peripheral (3, 8, and 12 N-substitution) and *meso*-positions of the macrocycle, which could help to generate supramolecular structures with fixed distances and orientation.[7−11] This would allow a comparison between the electrochemistry of monomeric Ni(II) chlorins and that of the corresponding dyads linked by one or three double bonds at the *meso*-position or peripheral position to give fixed orientations. Finally, we have previously shown that certain biologically inactive porphyrin monomers have enhanced in vivo efficacy when converted into the corresponding dimers with carbon−carbon linkages between the two macrocycles.[12,13] Thus, there was a good possibility that single purpurinimides having long wavelength absorption (700 nm) and high singlet oxygen producing efficiency (>50%) might show improved photodynamic therapy (PDT) efficacy upon conversion to the corresponding dimers (nonmetallated analogs). Finally, it was thought that under controlled conditions the McMurry approach might be useful in developing heterodimers joined with C−C linkages.

The utility of the McMurry reaction in porphyrin chemistry has been explored in depth by Vicente and Smith,[14] who showed that metalloformylporphyrins, metallo(2-formylvinyl)porphyrins, and chlorins upon reacting with $TiCl_3(DME)_{1.5}$−Zn(Cu) could be efficiently dimerized, giving bismacrocyclic compounds, which were linked with either one or three carbon−carbon double bonds. This approach was further extended to the pyropheophorbide system to obtain planar bischlorin derivatives with a completely conjugated π system.[15] This coupling approach has also been used by Vogel and co-workers in the preparation of the porphycene class of pyrrole macrocycles.[16] Interestingly, our reaction of purpurinimide analogs containing a formyl or 2-formylvinyl substituent with $TiCl_3(DME)_{1.5}$−Zn(Cu) did not produce the desired dimers. Instead, the formyl derivatives were found to be inactive, whereas the 2-formylvinyl analogs produced benzoisobacteriopurpurinimides as the main products via intramolecular cyclization. However, following the modified McMurry reaction conditions ($TiCl_4$−Zn) reported by Mukaiyama et al.,[17] the reaction afforded the dimeric species in modest yields.

Results and Discussion

For preparation of dimers with variable carbon linkages joined either at the *meso*-position or peripheral position, purpurin-18-N-hexylimide **1** was used as a substrate, which in turn was obtained from methyl pheophorbide-*a* by following the literature procedure.[18] The reaction of **1** with $Ni(acac)_2$ and subsequent treatment with Pd/C under a hydrogen atmosphere afforded Ni(II) mesopurpurin-18-N-hexylimide **3** in almost quantitative yield, which upon further treatment with $POCl_3$/DMF under Vilsmeier reaction conditions, produced 20-*meso*-formyl analog **4** in excellent yield. Under similar reaction conditions, the reaction of **3** with 3-(dimethylamino) acrolein and phosphoryl chloride (3-DMA/$POCl_3$) produced the corresponding 20-formylvinylpurpurinimide **5** in 75% yield (Scheme 1). 20-Formylpurpurinimide **4**, upon being subjected to the reductive coupling reaction under conditions reported by Vicente and Smith[14] [the active titanium reagent was prepared by refluxing a slurry containing 9.9 equiv of $TiCl_3(DME)_{1.5}$ and 35.5 equiv of Zn−Cu couple for 2 h in 1,2-dimetoxyethane (DME)], did not form the expected dimers. Instead, the starting *meso*-formyl compound **4** was isolated almost quantitatively, whereas the formylvinyl analog produced isobacteriopurpurinimide **6** as a sole product. Subjecting the purpurinimide **10** to the reductive coupling reaction, in which the N-hexyl group was replaced with the 3,5-bis(trifluoromethyl) benzyl group using a similar McMurry reaction condition, afforded the cyclic products **11** (major) and **12** (minor), in which the acrolein group cyclized onto the adjacent pyrrole subunit (Scheme 2). Leaving the reaction continue for a longer time produced mainly the isobenzochlorin analog **11**. The structures of both cyclic products were confirmed by comparative ^{1}H NMR studies (Figure 1).

The formation of such a cyclic structure from the *meso*-(2-formylvinyl)-substituted porphyrins via acid-catalyzed conditions has previously been reported by us[19−22] and others.[23−28]

(3) Ephritikhine, M. *Chem. Commun.* **1998**, 2549–2554.
(4) Ohkubo, K.; Kotani, H.; Shao, J.; Ou, Z.; Kadish, K. M.; Li, G.; Pandey, R. K.; Fujitsuka, M.; Ito, O.; Imahori, H.; Fukuzumi, S. *Angew. Chem., Int. Ed.* **2004**, *43*, 853–856.
(5) Fukuzumi, S.; Ohkubo, K.; Imahori, J.; Shao, J.; Ou, Z.; Zheng, G.; Chen, Y.; Pandey, R. K.; Fujitsuka, M.; Ito, O.; Kadish, K. M. *J. Am. Chem. Soc.* **2001**, *123*, 10676.
(6) Ohkubo, K.; Imahori, H.; Shao, J.; Ou, Z.; Kadish, K. M.; Chen, Y.; Zheng, G.; Pandey, R. K.; Fujitsuka, M.; Ita, O. *J. Phys. Chem. A* **2002**, *106*, 10911.
(7) Deisenhofer, J., Norris, J. R., Eds. *The Photosynthetic Reaction Center*; Academic Press: San Diego, 1993.
(8) Verhoeven, J. W. *Adv. Chem. Phys.* **1999**, *106*, 603.
(9) Osuka, A.; Mataga, N.; Okada, T. *Pure Appl. Chem.* **1997**, *69*, 797.
(10) Lewis, F. D.; Letsinger, R. L.; Wasieleweski, M. R. *Acc. Chem. Res.* **2001**, *34*, 159.
(11) Gust, D.; Moore, T. A. In *The Porphyrin Handbook*; Kadish, K. M., Smith, K. M., Guilard, R., Eds.; Academic Press: San Diego, 2000; *Vol. 8*, p 153.
(12) Pandey, R. K.; Smith, K. M.; Dougherty, T. J. *J. Med. Chem.* **1990**, *33*, 2032.
(13) Pandey, R. K.; Shiau, F.-Y.; Medforth, C.; Dougherty, T. J.; Smith, K. M. *Tetrahedron Lett.* **1990**, *31*, 789, and references cited therein.
(14) Vicente, M. G. H.; Smith, K. M. *J. Org. Chem.* **1991**, *56*, 4407.
(15) (a) Jaqinod, L.; Nurco, D. J.; Medforth, C. J.; Pandey, R. K.; Forsyth, T. P.; Olmstead, M. N.; Smith, K. M. *Angew. Chem., Int. Ed. Engl.* **1996**, *35*, 1013. (b) Jaquinod, L.; Senge, M. O.; Pandey, R. K.; Forsyth, T. P.; Smith, K. M. *Angew. Chem., Int. Ed. Engl.* **1996**, *35*, 1840.
(16) Vogel, E.; Kocher, M.; Schmickler, H.; Lex, J. *Angew. Chem., Int. Ed. Engl.* **1988**, *26*, 267.
(17) Mukaiyama, T.; Sato, T.; Hanna, J. *Chem. Lett.* **1973**, 1041.
(18) Gryshuk, A.; Chen, Y.; Goswami, L. N.; Pandey, S.; Missert, J. R.; Ohulchanskyy, T.; Potter, W.; Prasad, P. N.; Oseroff, A.; Pandey, R. K. *J. Med. Chem.* **2007**, *50*, 1754.
(19) Mettath, S. N.; Shibata, M.; Alderfer, J.; Senge, M. O.; Smith, K. M.; Rein, R.; Dougherty, T. J.; Pandey, R. K. *J. Org. Chem.* **1998**, *63*, 1646.
(20) Mettath, S. N. Synthesis of New Photosensitizer and their Biological Significance. Ph.D. Thesis, Roswell Park Cancer Institute, SUNY, Buffalo, NY, 1999.
(21) Meunier, I.; Pandey, R. K.; Senge, M.; Dougherty, T. J.; Smith, R. K. *Bioorg. Med. Chem. Lett.* **1992**, *2*, 1575.
(22) Pandey, R. K.; Jagerovic, N.; Ryan, J. M.; Dougherty, T. J.; Smith, K. M. *Bioorg. Med. Chem. Lett.* **1993**, *3*, 2615.
(23) Smith, K. M.; Bisset, G. M. F.; Tabba, H. D. *J. Chem. Soc., Perkin Trans. 1* **1982**, 581.
(24) Morgan, A. R.; Skalkos, D.; Maguire, G.; Ramprasaud, A.; Garbo, G.; Keck, R. W.; Selman, S. H. *Photochem. Photobiol.* **1992**, *55*, 133.
(25) Arnold, D. P.; Holmes, R. G.; Johnson, A. W.; Smith, A. R. P.; Williams, G. A. *J. Chem. Soc., Perkin Trans. 1* **1978**, 1660.

SCHEME 1. Synthesis of *meso*-Substituted Formyl and 2-Formylvinyl Purpurinimides

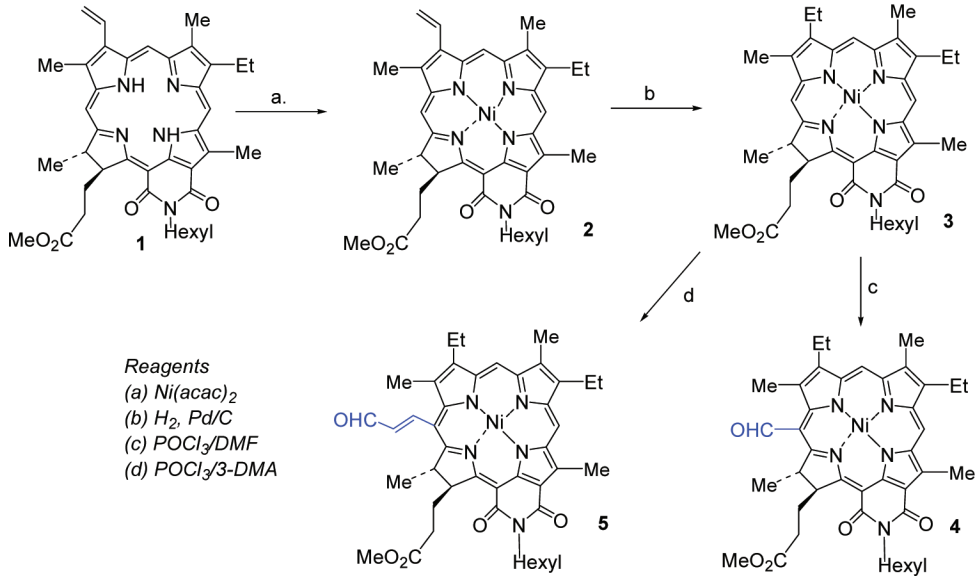

SCHEME 2. Intramolecular Cyclization of 20-*meso*-2-Formylvinylpurpurinimide under McMurry Reaction Conditions Using $TiCl_3(DME)_{1.5}$−Zn(Cu) Combination

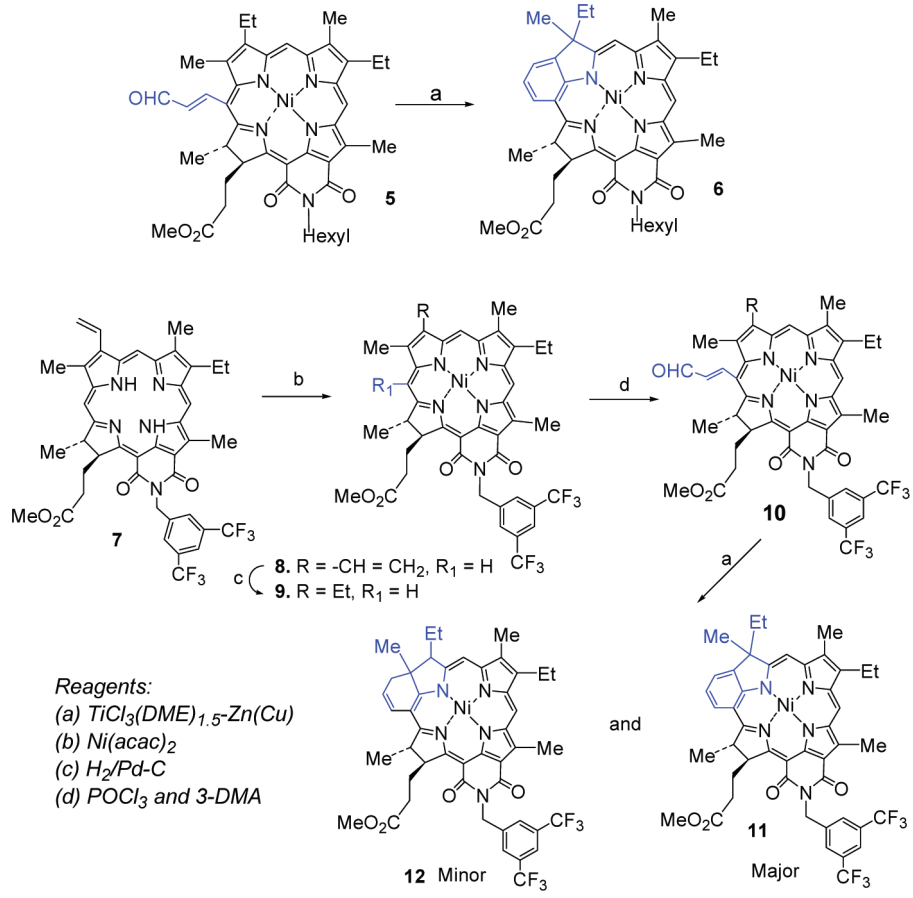

However, this is the first example showing the utility of the McMurry reaction for the preparation of a novel new benzoisobacteriochlorin system.

For the preparation of the desired purpurinimide dyads (homodimers), the 3-formyl- and 2-formylvinyl purpurinimides were individually subjected to various modified McMurry reaction conditions, and interestingly, upon treating 20-formyl-*meso*-purpurinimide **4** with $TiCl_4$/Zn, the desired dimer with one carbon−carbon bond **13** was obtained in 42% yield. In the NMR spectrum, the alkene protons appear as a singlet at 7.09 ppm, indicating that they are magnetically equivalent, and that the dimer molecule has an element of symmetry. Under similar conditions, the reaction of 20-formylvinyl purpurinimide **5** afforded dimer **15**, containing a hexatriene linker as a major product. The 2-formyl vinyl group (−CH═CH−CHO) in compound **5** consists of a *trans*-conformation. Therefore, the

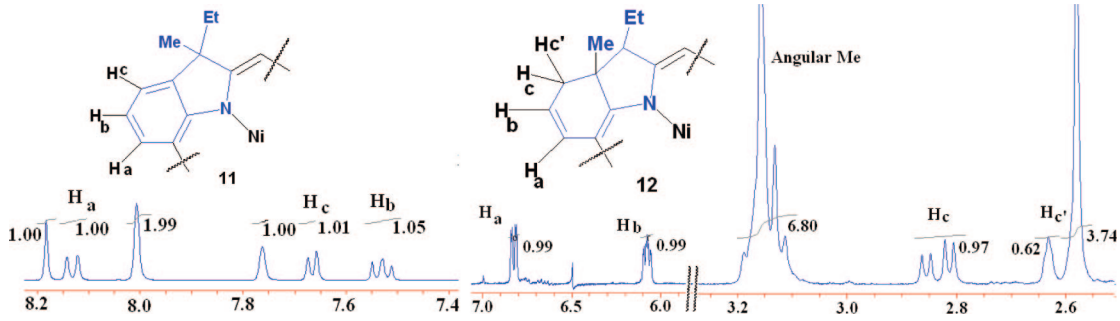

FIGURE 1. Partial NMR spectra of benzoisobacteriopurpurinimdes **11** and **12**.

SCHEME 3. Synthesis of Carbon−Carbon-Linked Purpurinimide Dimers via Modified McMurry Reaction Using $TiCl_4$−Zn Combination

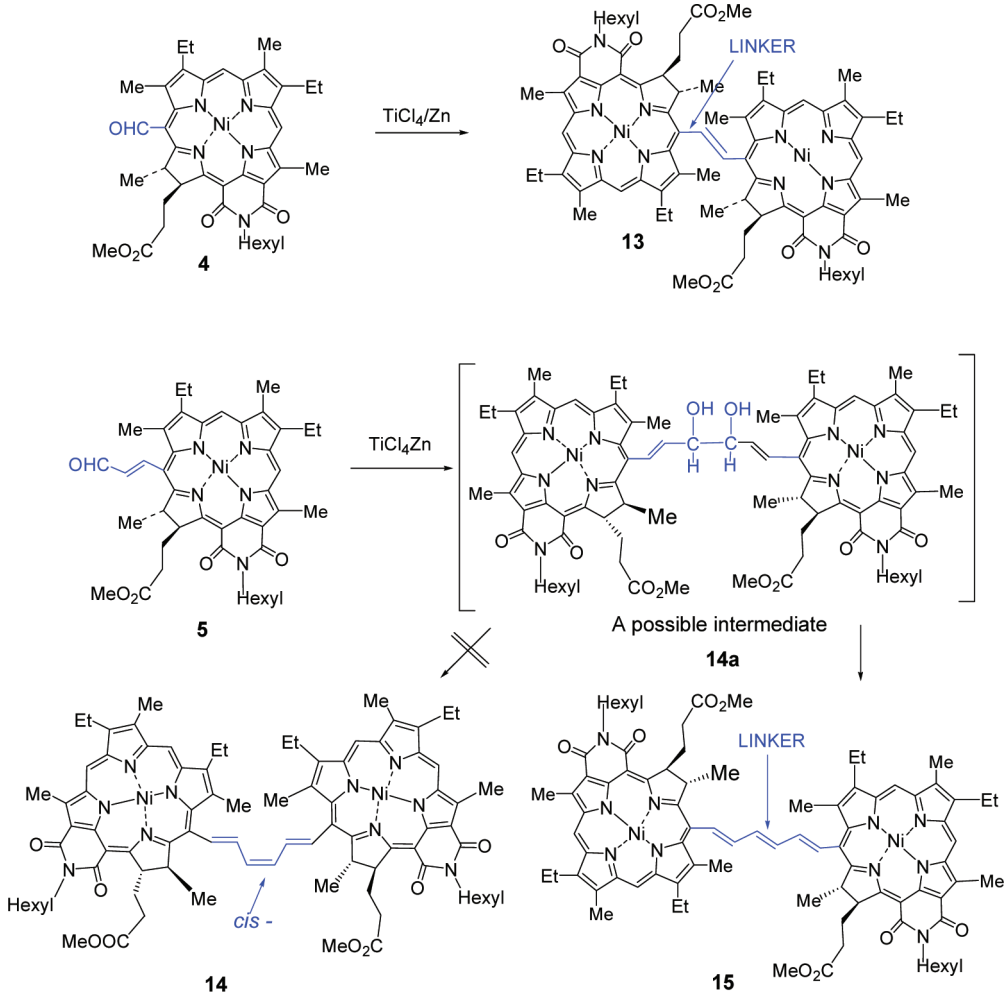

resulting dimer **15** (Scheme 3) with a triene linkage could exist in either *EEE* or *EZE* isomer forms. The NMR analyses of **15** clearly indicate its symmetrical nature, and the coupling constant values of the triene protons were found to be 15.0, 6.8, and 2.8 Hz, which correspond to the J_{ab}, J_{bc}, and J_{ac} values of the triene, respectively. Because the molecule is symmetrical, these values are also equal to $J_{a'b'}$, $J_{b'c'}$, and $J_{a'c'}$, respectively, which reflects the structure having a *trans, trans*, and *trans* geometry and agrees with the similar triene system reported in the literature.[14,29]

The molecular modeling study also indicated that an all *trans* configuration is more stable than a *trans-cis-trans* configuration from the selected conformations examined for the dimer connected at the *meso-* position. Because there are many rotational degrees of freedom for the six-carbon linker region, it was not possible to examine all possible conformations. In general, the semiempirical MO used in this study tends to underestimate the conformational energy differences, but nevertheless, the all *trans* configuration is about 4 kcal/mol more stable than the *trans-cis-trans* configuration. The energy-

(26) Gunter, M. J.; Robinson, B. C.; Gulbis, J. M.; Tiekink, R. T. *Tetrahedron* **1991**, *47*, 7853.
(27) Osuka, A.; Hoshiya, I.; Maruyama, K. *Bull. Chem. Soc. Jpn.* **1992**, *65*, 3322.
(28) Boyle, R. W.; Dolphin, D. *J. Chem. Soc., Chem. Commun.* **1994**, 2463.
(29) Sonoda, Y.; Nakao, Y. *J. Chem. Soc., Perkin Trans. 1* **1993**, 1147.

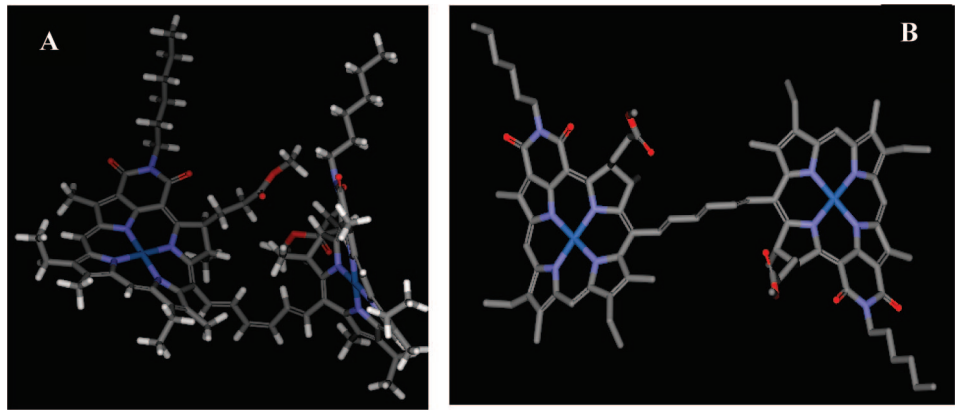

FIGURE 2. Energy-optimized structures of (A) dimer **14** containing a *trans-cis-trans* and (B) dimer **15** containing a *trans-trans-trans* hexatriene linker.

SCHEME 4. *β*−*β*-Linked Purpurinimides with One and Three Double Bonds

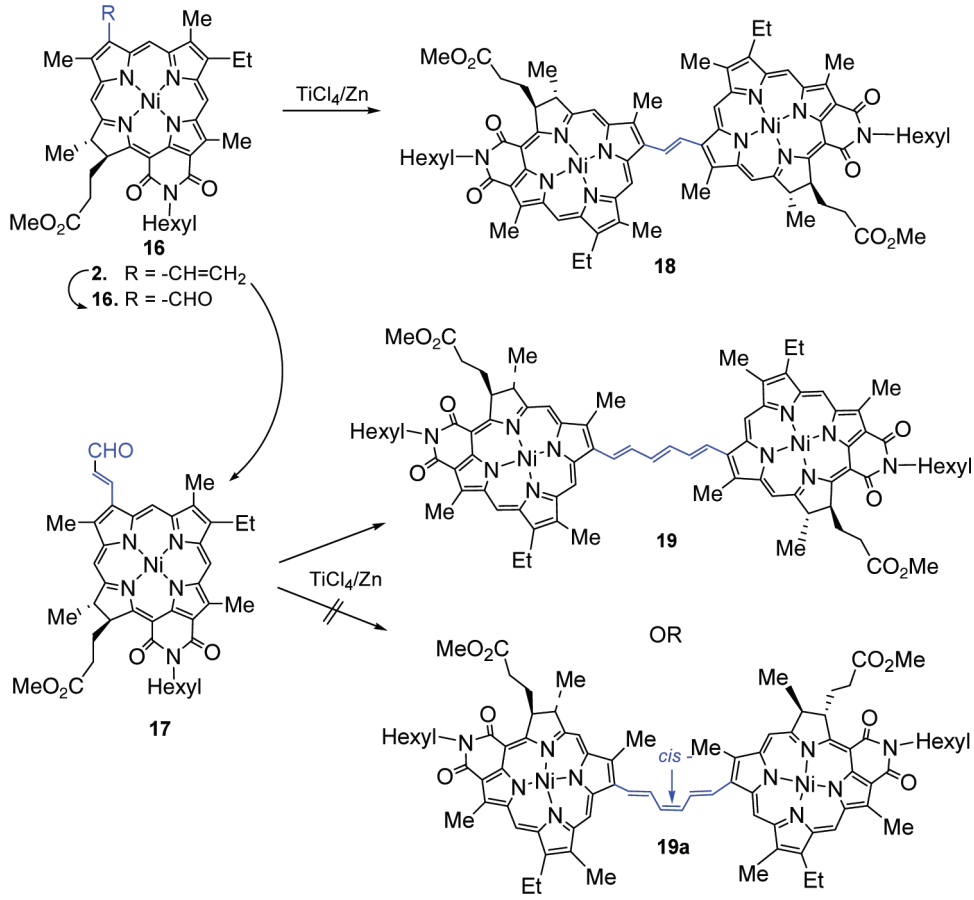

optimized structures of a possible conformer for all *trans* and *trans-cis-trans* configurations of the hexatriene in dimer **14** and **15**, respectively, are in Figure 2.

For the preparation of *β*−*β*′-linked purpurinimides with one and three double bond carbon units, Ni(II) 3-formylpurpurin-18-N-hexylimide **16** and 3-2′-formylvinyl-purpurin-18-N-hexylimide **17** were used as substrates and were obtained by reacting Ni(II) purpurinimide **2** with osmium tetroxide/sodium periodate[30] and $POCl_3$/DMF, respectively. Reaction of the formyl analogs with $TiCl_4$/Zn in THF for 30−45 min produced dimers **18** and **19** in excellent yields (Scheme 4). Compared to the dimers connected at the *meso*-positions, slightly different trends were observed by the molecular modeling study for dimers connected at a *β*-pyrrole position. Again, all possible conformations were not examined, but those selected conformations examined for dimers **19** and **19a** are in Figure 3. Among the seven conformers examined (three all *trans* configurations and four *trans-cis-trans* configurations), the maximum energy difference was only 2 kcal/mol indicating very similar stabilities among the different conformers. Although the most stable conformer belongs to the all *trans* configuration, other conformers in all *trans* configurations were very similar in stability to

(30) Li, G.; Dobhal, M. P.; Shibata, M.; Pandey, R. K. *Org. Lett.* **2004**, *6*, 2393.

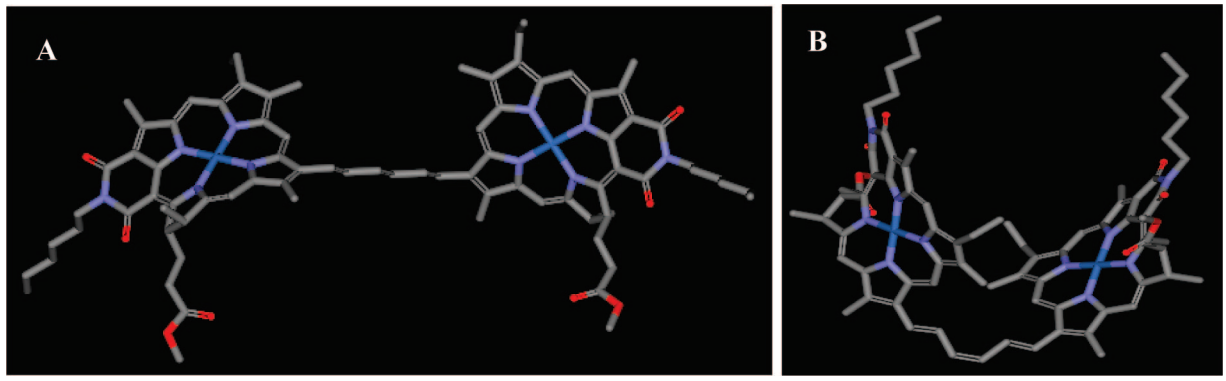

FIGURE 3. Energy-minimized structures of $\beta-\beta$-linked dimers with a hexatriene linker: (A) *trans-trans-trans* configuration **19** and (B) *trans-cis-trans* configuration **19a**.

TABLE 1. Half-Wave Potentials (V vs SCE) of Investigated Nickel Chlorins in PhCN and 0.1 M TBAP

	linker[a]		oxidation			reduction				
compound	position	"type"	second	first		first		second		HOMO−LUMO[b]
3	none		1.11	0.81			−0.99		−1.43	1.80
13	*meso*	short	1.19	0.84		−0.85	−0.95		−1.42	1.69
18	β	short	1.14	0.87		−0.84	−0.94	−1.30	−1.48	1.71
15	*meso*	long	1.20	0.88	0.70		−0.92		−1.39	1.62
19	β	long	1.16	0.83	0.76		−0.89	−1.24	−1.35	1.65

[a] See Schemes 1, 3, and 4 for structures. [b] $\Delta E_{1/2}$ between first reduction and first oxidation.

conformers belonging to the *trans-cis-trans* configuration. Thus, from the molecular modeling study alone, it is not possible to decide the conformation of the linker regions in dimers formed through linking at the β-position. It is speculated that dimer formation through the *meso*-position will create a tighter steric hindrance than that for the corresponding dimer linked through the β-positions. This in turn restricts the number of possible conformers. From the very similar energies for various conformers in dimers connected through the β-position, it is concluded that the nature of conformational energy difference found in all *trans* vs *trans-cis-trans* conformers for both the dimers connected at the *meso*- or β-position is not because of the intrinsic conformational energy difference of the linker region, which is identical for both dimers.

Redox Processes. The electrochemistry of Ni(II) purpurinimide **3** and the corresponding dyads **13**, **15**, **18**, and **19** was investigated in benzonitrile (PhCN) containing 0.1 M TBAP as the supporting electrolyte. Half-wave potentials for each process of the five compounds are given in Table 1, and cyclic voltammograms (CV) of each in PhCN and 0.1 M TBAP are in Figure 4.

Monomeric nickel chlorin **3** (top CV in Figure 4) undergoes two reversible one-electron reductions at $E_{1/2} = -0.99$ and -1.43 V and two reversible one-electron oxidations at $E_{1/2} =$ 0.81 and 1.11 V. A global addition or abstraction of two electrons also occurs for each macrocycle of the four electrochemically characterized dyads, with the potentials of each process varying with both the position and type of linkage. This is seen from the data in Table 1 where the two dyads with short linkers at the *meso*-position (**13**) or β-pyrrole position (**18**) of the macrocycle are both more difficult to oxidize than the monomeric chlorin **3** by 30−60 mV and easier to reduce by 140−150 mV. Compounds **13** and **18** also exhibit separate half-wave potentials for the first electron addition to each macrocycle, one process occurring at −0.84 to −0.85 V and the other at −0.94 to −0.95 V (Table 1). Dyads **13** and **18** have a similar HOMO−LUMO gap of 1.69−1.71 V as compared to 1.80 V for monomeric chlorin **3**.

In contrast to the above dyads with short linkers, those with long *meso* (**15**) or β-pyrrole (**19**) linking groups are both easier to reduce and easier to oxidize than monomer **3**. The difference in potential is 70−100 mV on reduction and 50−110 mV on oxidation, which leads to a smaller HOMO−LUMO gap of 1.62−1.65 V for dyads with the long linkers as compared to 1.65−1.71 V for dyads **13** and **18** with the short linkers and 1.80 V for monomeric chlorin **3**. The two macrocycles of dyads **15** and **19** are reduced at the same half-wave potential, indicating a lack of interaction between the two conjugated π systems, but this is not the case for oxidation where the two equivalent macrocycles show separate processes for the first electron abstraction, these reactions occurring at $E_{1/2} = 0.70$ or 0.76 V and 0.83 or 0.88 V as seen in Table 1 and Figure 4.

An interaction between the two doubly reduced macrocycles of **18** and **19** is also seen in the cyclic voltammograms of Figure 4. This is most clearly illustrated in the CV of **18** where the reversible addition of a second electron to the two linked macrocycles of the dyad occurs at −1.30 and −1.48 V as compared to $E_{1/2} = -1.43$ V in the case of compound **3**. The currents for the "split" second reduction of **18** at −1.30 and −1.48 V are about half of that for the compound's single oxidation at 0.87 V, and this is consistent with the global addition and abstraction of one electron per macrocycle in each case.

Spectroelectrochemical data indicate that the first electron addition and first abstraction of the five electrochemically characterized dyads involves the conjugated macrocycle, and no metal-centered reactions are observed. This is discussed below.

UV−Visible Spectra of Neutral, Electrooxidized, and Electroreduced Compounds. Three types of UV−visible spectra were obtained for the investigated compounds. One is for monomeric chlorin **3**, and the other two are for dyads with

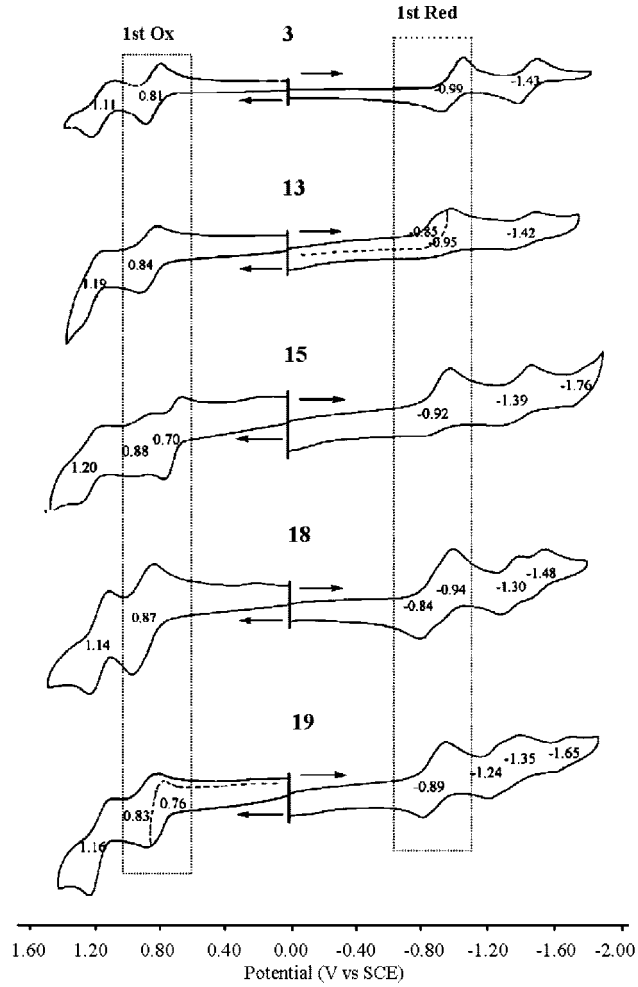

FIGURE 4. Cyclic voltammograms of monomeric chlorin **3** and dyads with "short" (**13**) or "long" (**15**) *meso* linkers and "short" (**18**) or "long" (**19**) β-pyrrole linkers in PhCN, containing 0.1 M TBAP. Scan rate = 0.10 V/s.

TABLE 2. UV−Visible Spectral Data of Neutral Nickel Chlorins in PhCN Containing 0.1 M TBAP

		λ_{max}, nm ($\varepsilon \times 10^{-4}$, mol^{-1} cm^{-1})				
linker	compound	Soret region		visible region		
none	**3**	393 (3.5)	421 (6.1)	544 (0.4)	615 (0.95)	664 (3.3)
meso	**13**	363 (4.9)	429 (10.9)	581 (1.1)		695 (6.3)
	15	363 (2.8)	431 (6.6)	581 (0.8)		700 (3.6)
β-pyrrole	**18**	392 (8.6)	424 (13.1)	556 (1.4)	677 (5.5)	714 (7.2)
	19	391 (5.1)	425 (8.7)	560 (1.3)	683 (3.8)	716 (5.3)

meso or β-pyrrole linkers, either long or short as seen in Table 2. Monomeric compound **3** has a split Soret band at 421 and 393 nm, an intense visible band at 664 nm, and two additional bands at 544 and 615 nm. All four dyads have a split Soret band, and the main difference between spectra of these compounds is in the visible region where *meso*-linked **13** and **15** are characterized by two bands at 581 and 695−700 nm and β-pyrrole-linked **18** and **19** are characterized by three bands between 556 and 716 nm as seen in Table 2. No major difference in the position of the bands for the neutral compounds is seen upon changing the length of the linker, i.e., between **13** (short) and **15** (long) or between **18** (short) and **19** (long), and this is also the case after the global addition or abstraction of one electron per macrocycle in a thin-layer spectroelectrochemical cell.

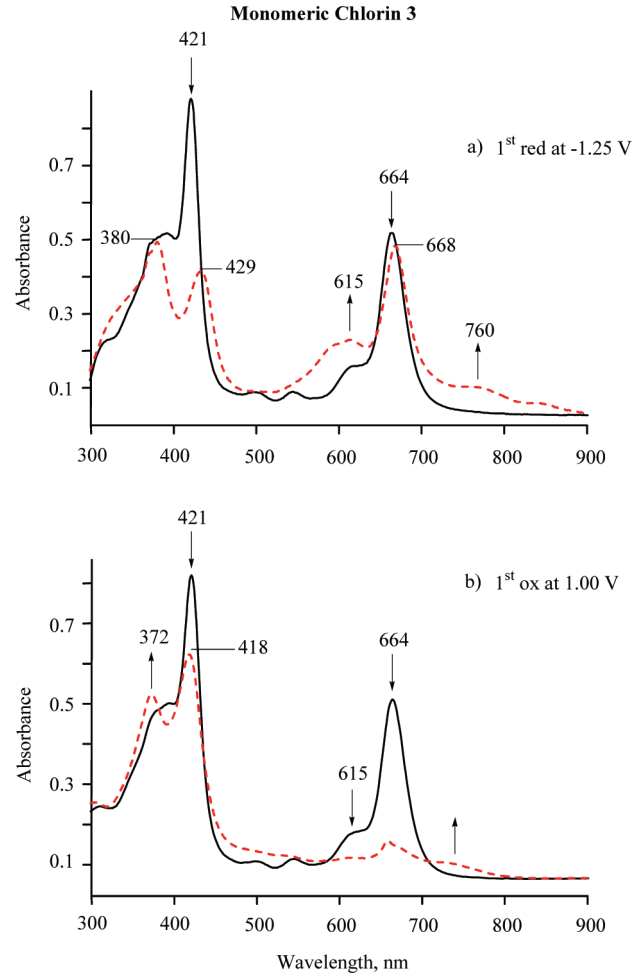

FIGURE 5. UV−visible spectral changes of compound **3** in PhCN containing 0.2 M TBAP during the first reduction and the first oxidation processes. The solid lines correspond to the absorption spectra of the neutral compounds.

In order to investigate the site of electron transfer and/or degree of interaction between the two macrocycles in their oxidized and reduced forms, UV−visible spectra of each compound were obtained in a thin-layer cell after oxidation and reduction at a controlled potential. Examples of the spectral changes are in Figures 5−7 for monomeric chlorin **3**, along with the two sets of dyads with long or short linkers at the *meso*-position or β-pyrrole position of the macrocycle.

Applying a reducing potential of −1.25 V to a solution of compound **3** in PhCN containing 0.2 M TBAP leads to a decrease in the initial Soret band in intensity as a new species is formed which has a split Soret band at 380 and 429 nm (Figure 5a). The initial visible band at 664 nm decreases only slightly in intensity upon reduction and is red-shifted to 668 nm, but two new visible bands of the reduced product appear at 615 and 760 nm, suggesting formation of a π-anion radical during the first one-electron reduction. A split Soret band is also seen after oxidation of **3** at 1.00 V, and under these conditions, major changes occur in the visible region of the spectrum. The spectra of the oxidized species are shown by the dashed red line in Figure 5b. The intense visible band of the neutral compound at 664 nm is no longer present and is replaced by a broad low-intensity absorption between 700 and 800 nm. This type of spectrum suggests a π-cation radical for the singly oxidized chlorin.

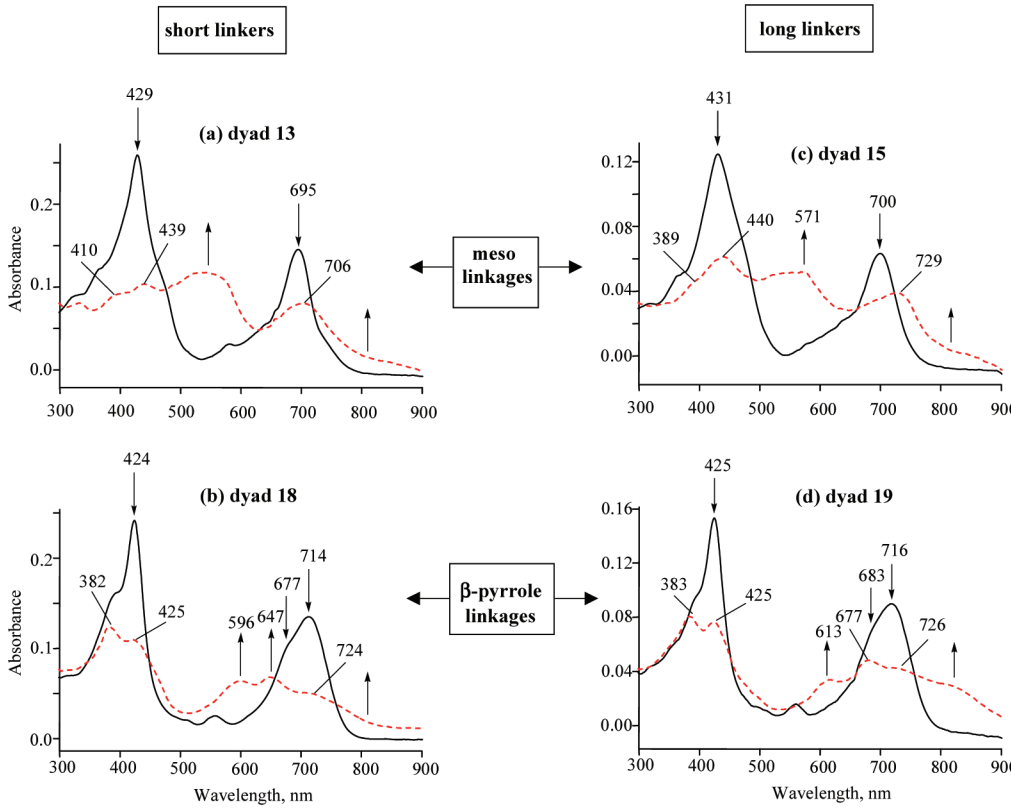

FIGURE 6. UV−visible spectral changes during a global one-electron reduction of the four dyads at an applied potential of −1.10 V in PhCN containing 0.2 M TBAP. The solid lines correspond to the absorption spectra of the neutral compounds.

The global addition or abstraction of one electron to each macrocycle of dyads **13**, **15**, **18**, and **19** also produces UV−visible spectra characteristic of π-anion radicals (reduction) and π-cation radicals (oxidation). The final spectra of the electroreduced and electrooxidized products are in red in Figures 6 and 7 where comparisons of the dyads can be made either as a function of the length of the linker, short (two left spectra) or long (two right spectra), or as a function of the linker position (*meso*-linked dyads at the top of figures and β-linked dyads at the bottom).

As indicated previously, the major difference in UV−visible spectra of the neutral dyads depends upon the position of the linkage and not the length of the linkers (see black spectra of neutral compounds in Figures 6 and 7), and the same can be said after the addition or abstraction of one electron where the product of the electron transfer reaction is drawn in red in the two figures.

The two singly reduced dyads with *meso*-linkages have five bands between 350 and 850 nm, while those with β-pyrrole linkages have six bands over the same spectral region. Like the spectrum of singly reduced compound **3**, there is a split Soret band, but unlike compound **3**, the initial Q-band is significantly decreased in intensity, suggesting a π-anion radical in each case. The different spectra for monomeric **3** and the four dyads after reduction may be related to interactions, which occur between the two anion radicals in each dyad as is evident from the cyclic voltammograms in Figure 4.

Fewer differences are seen in UV−visible spectra of the electrooxidized dyads, and unlike the case of reductions, the final spectra (Figure 7, red lines) closely resemble the spectrum of singly oxidized compound **3** under the same solution conditions (Figure 5b, red line). In each case, the singly oxidized dyads have a split Soret band, and the spectra are similar to that of a π-cation radical where one electron is abstracted from each macrocycle of the dyad.

Conclusion

The McMurry reaction provides a unique opportunity to prepare porphyrin-based dimers with fixed orientations. The nature of the titanium reagent shows a strong influence on the eventual formation of the cyclic or dimeric structures and stereochemistry. Poor quality reagents or solvents or the introduction of air results in poor yields of the desired products. An involvement of pinacolate intermediates in the McMurry reaction for the formation of purpurinimide dimers seems to occur as noted in other systems. Each investigated dyad shows behavior similar to that of the monomeric unit, but changes in the length or position of the linker can result in changes in the electrochemical and spectroelectrochemical properties of the compounds and/or the extent of interaction between the neutral, electroreduced, or electrooxidized species. There is no significant difference in UV−visible spectra between the *meso*- and β-linked dyads as a function of the spacer length, but the length of the spacer does affect the ease of oxidation and reduction, the resulting HOMO−LUMO gap, and the interaction between the two oxidized or reduced units.

Experimental Section

All reactions were carried out in flame-dried glassware under an atmosphere of nitrogen with magnetic stirring. Thin-layer chromatography (TLC) was performed on Analtech precoated silica

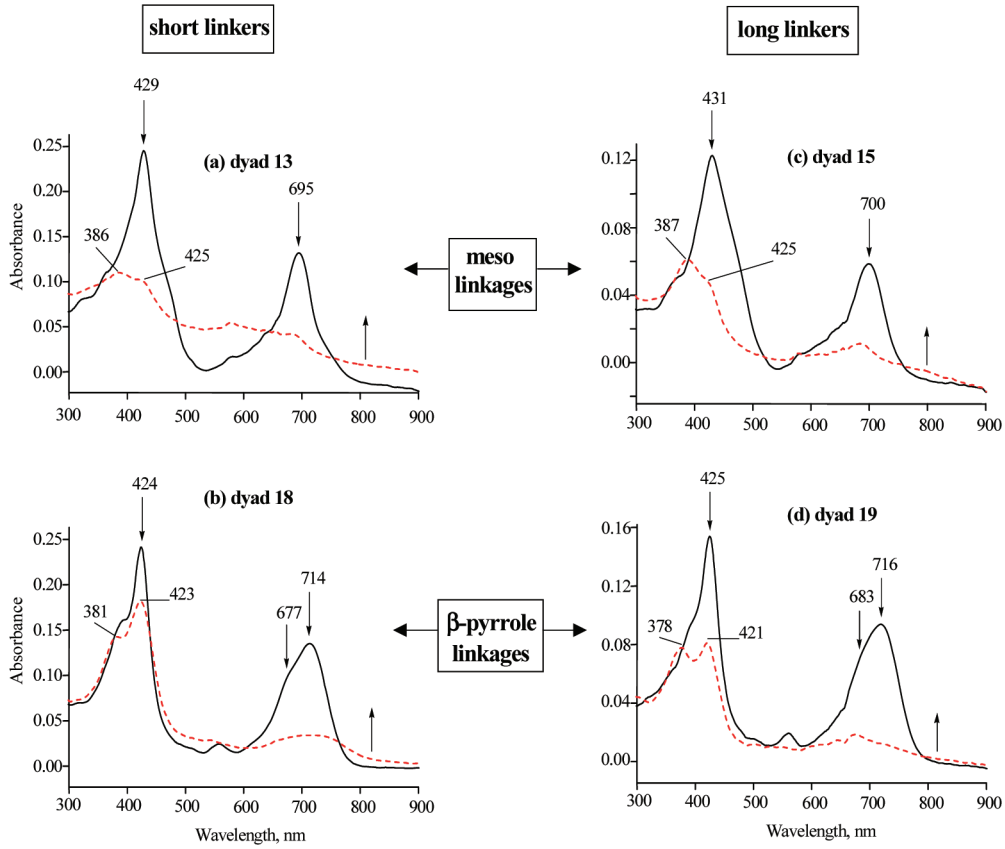

FIGURE 7. UV−visible spectral changes during a global one-electron oxidation of the four dyads at an applied potential of 1.00−1.10 V in PhCN containing 0.2 M TBAP. The solid lines correspond to the absorption spectra of the neutral compounds.

gel GF PE sheets (catalog no. 159017, layer thickness 0.25 mm) and aluminum oxide NF PE sheets (catalog no. 101016, layer thickness 0.2 mm). Column chromatography was performed either over silica gel 60 (70−230 mesh) or neutral alumina (Brockmann grade III, 50 mesh). In some cases preparative TLC plates were also used for the purification (Analtech precoated silica gel GF glass plate, catalog no. 02013, layer thickness 1.0 mm). Solvents were purified as follows: trace amounts of water and oxygen from THF were removed by refluxing over sodium under an inert atmosphere. Dichloromethane was dried over P_2O_5. Anhydrous DMF, triethylamine, pyridine, and other common chromatographic solvents were obtained from commercial suppliers (J. T. Baker, EMD, and Aldrich) and used without further purification. NMR spectra were recorded on a Bruker DRX 400 MHz spectrometer. All chemical shifts are reported in parts per million (δ). ^{1}H NMR (400 MHz) spectra were recorded at rt in $CDCl_3$ or CD_3OD solutions and referenced to residual $CHCl_3$ (7.26 ppm) or TMS (0.00 ppm). ^{1}H NMR data of the symmetrical dimers are given as their monomer half. EI-Mass spectra were recorded on a Brucker Esquire ion-trap mass spectrometer equipped with a pneumatically assisted electrospray ionization source, operating in positive mode. The high-resolution mass spectrometry analyses were performed at the Mass Spectrometry Facility, Michigan State University. UV−visible spectra were recorded on a Varian Cary 50 Bio UV−visible spectrophotometer using dichloromethane as solvent. All photophysical experiments were carried out using spectroscopic grade solvents.

Ni(II)-Purpurin-18-N-hexylimide Methyl Ester (2). Purpurin-18-N-hexylimide **1** (610.0 mg, 0.92 mmol) was dissolved in 100 mL of toluene, and nickel acetylacetonate hydrate (2.36 mg, 9.2 mmol) was added to it. The reaction mixture was refluxed vigorously for 2 h, and progress of the reaction was monitored by TLC and UV−visible spectroscopy. After completion, the reaction mixture was cooled and filtered through a Celite bed, and then the filtrates were concentrated and directly loaded onto a silica column. Product **2** was eluted with a 1% acetone/dichloromethane mixture. Yield: 600.0 mg (90.6%). UV−vis λ_{max} (in CH_2Cl_2): 673 nm (ε 4.1 × 10^4), 548 nm (ε 0.5 × 10^4), 423 nm (ε 6.9 × 10^4), 379 nm (ε 3.9 × 10^4). ^{1}H NMR (400 MHz, $CDCl_3$): δ 9.02 (s, 1H, *meso*-H), 8.77 (s, 1H, *meso*-H), 7.93 (s, 1H, *meso*-H), 7.58 (dd, 1H, 3-C<u>H</u>=C<u>H</u>$_2$, J = 11.6 and 17.6 Hz), 5.92 (dd, 2H, 3-CH=C<u>H</u>$_2$, J = 9.6 and 15.6 Hz), 4.79 (dd, 1H, 17-H, J = 3.2 and 8.8 Hz), 4.28 (m, 2H, N-CH_2-hexyl), 4.07 (q, 1H, 18-H, J = 6.8 Hz), 3.61 (s, 3H, CO_2Me), 3.50 (s, 3H, ring-CH_3), 3.46−3.38 (m, 2H, 8-C<u>H</u>$_2$CH$_3$), 3.00 (s, 3H, ring-CH_3), 2.95 (s, 3H, ring-CH_3), 2.65−2.61 (m, 1H, 17^2-C<u>H</u>H), 2.59−2.55 (m, 1H, 17^2-CH<u>H</u>), 2.22−2.20 (m, 1H, 17^1-C<u>H</u>H), 1.95−1.93 (m, 1H, 17^1-CH<u>H</u>), 1.88−1.83 (m, 2H, CH_2-hexyl), 1.55−1.49 (m, 5H, 8-CH_2C<u>H</u>$_3$ and -CH_2-hexyl), 1.45−1.37 (m, 4H, 2CH_2-hexyl), 1.34 (d, 3H, 18-CH_3, J = 7.2 Hz), 0.93 (t, 3H, CH_3-hexyl, J = 6.8 Hz). EIMS (*m*/*z*): 741 (M^+ + Na). HRMS: calcd for $C_{40}H_{45}N_5NiO_4$ 717.2825, found 717.2815.

Ni(II)-*meso*-Purpurin-18-N-hexylimide Methyl Ester (3). Ni(II)-3-(Vinyl)-purpurin-N-hexylimide **2** (350.0 mg, 0.48 mmol) was dissolved in 100 mL of distilled THF. Pd/C (10% w/w, 350.0 mg) and 5 or 6 drops of triethylamine were added to the reaction mixture. The reaction mixture was degassed, flushed with H_2, and stirred vigorously for 12 h under H_2 atmosphere. Progress of the reaction was monitored by UV−vis and ^{1}H NMR. After completion of the reaction, the mixture was degassed, flushed with N_2, and filtered over a Celite bed. The filtrate was concentrated, and the crude product purified over a silica column using a 0.5−1% acetone/dichloromethane mixture as eluent. Yield: 300.0 mg (85.4%). UV−vis λ_{max} (in CH_2Cl_2): 661 nm (ε 3.2 × 10^4), 544 nm (ε 0.4 × 10^4), 501 nm (ε 0.4 × 10^4), 419 nm (ε 6.0 × 10^4). ^{1}H NMR (400 MHz, $CDCl_3$): δ 8.99 (s, 1H, *meso*-H), 8.61 (s, 1H, *meso*-H), 7.86 (s, 1H, *meso*-H), 4.78 (dd, 1H, 17-H, J = 3.2 and 9.2 Hz), 4.27 (m, 2H, N-CH_2-hexyl), 4.03 (q, 1H, 18-H, J = 7.2 Hz), 3.60 (s,

3H, CO_2Me), 3.48 (s, 3H, ring-CH_3), 3.44−3.36 (m, 4H, 3-$\underline{CH_2}CH_3$ and 8-$\underline{CH_2}CH_3$), 2.95 (s, 3H, ring-CH_3), 2.87 (s, 3H, ring-CH_3), 2.64−2.54 (m, 2H, 17^2-CH_2), 2.20−2.18 (m, 1H, 17^1-C$\underline{H}$H), 1.94−1.92 (m, 1H, 17^1-CH$\underline{H}$), 1.87−1.82 (m, 2H, CH_2-hexyl), 1.55−1.48 (m, 8H, 3-$CH_2\underline{CH_3}$, 8-$CH_2\underline{CH_3}$, and CH_2-hexyl), 1.44−1.36 (m, 4H, $2CH_2$-hexyl), 1.33 (d, 3H, 18-CH_3, J = 6.8 Hz), 0.92 (t, 3H, CH_3-hexyl, J = 7.2 Hz). EIMS (*m*/*z*): 721 (M^+ + H). HRMS: calcd for $C_{40}H_{47}N_5NiO_4$ 719.2982, found 719.2971.

Ni(II)-20-*meso*-Formyl-*meso*-purpurin-18-N-hexylimide Methyl Ester (4). In a two-necked 100 mL dry round-bottomed flask, N,N′-dimethylformamide (1.0 mL) was dissolved in dry dichloromethane (20.0 mL), and the resultant mixture was cooled to 0 °C under N_2 atmosphere. To this cooled mixture was added $POCl_3$ (1.0 mL) slowly via syringe under continuous stirring. The reaction mixture was stirred for 20 min at the same temperature and then allowed to warm to rt. After 10 min, Ni-*meso*-purpurin-N-hexylimide **3** (100.0 mg, 0.13 mmol) in dry dichloromethane (15.0 mL) was added via syringe, and the resultant mixture was stirred for 36 h at rt. The reaction mixture was again cooled to 0 °C, and saturated Na_2CO_3 was added dropwise to the solution which was stirred for another 8 h. The reaction mixture was then extracted with dichloromethane (3 × 50.0 mL), and the organic layers were collected, combined, and washed with water (100.0 mL). The organic layer was separated, dried over anhydrous Na_2SO_4, and concentrated. The crude product thus obtained was purified over a silica column using a 1−2% acetone/dichlormethane mixture as eluent. Yield: 85.0 mg (82.5%). UV−vis λ_{max} (in CH_2Cl_2): 685 nm (ε 3.4 × 10^4), 426 nm (ε 3.5 × 10^4), 389 nm (ε 4.6 × 10^4). ^{1}H NMR (400 MHz, $CDCl_3$): δ 10.85 (s, 1H, -CHO), 8.70 (s, 1H, *meso*-H), 8.38 (s, 1H, *meso*-H), 4.80 (q, 1H, 17-H, J = 6.8 Hz), 4.53 (dd, 1H, 18-H, J = 4.8 and 8.8 Hz), 4.18 (q, 2H, N-CH_2-hexyl, J = 6.8 Hz), 3.63 (s, 3H, CO_2Me), 3.34 (s, 3H, ring-CH_3), 3.25 (m, 4H, 3-$\underline{CH_2}CH_3$ and 8-$\underline{CH_2}CH_3$), 2.83 (s, 3H, ring-CH_3), 2.82 (s, 3H, ring-CH_3), 2.64 (m, 2H, 17^2-CH_2), 2.17 (m, 1H, 17^1-CH_2), 1.88 (m, 1H, 17^1-CH_2), 1.77 (m, 2H, CH_2-hexyl), 1.50−1.43 (m, 8H, 3-$CH_2\underline{CH_3}$, 8-$CH_2\underline{CH_3}$, and CH_2-hexyl), 1.37 (m, 4H, $2CH_2$-hexyl), 1.14 (d, 3H, 18-CH_3, J = 6.8 Hz), 0.90 (t, 3H, CH_3-hexyl, J = 6.4 Hz). EIMS (*m*/*z*): 771 (M^+ + Na). HRMS: calcd for $C_{41}H_{47}N_5NiO_5$ 747.2931, found 747.2922.

Ni(II)-20-(2-Formylvinyl)-*meso*-purpurinimide-N-hexylimide Methyl Ester (5). In a two-necked 100 mL dry round-bottomed flask, 3-(dimethylamino)-acrolein (1.0 mL) was dissolved in dry dichloromethane (20.0 mL), and the resultant mixture was cooled to 0 °C under N_2 atmosphere. To this cooled mixture was added $POCl_3$ (1.0 mL) slowly via a syringe under continuous stirring. The reaction mixture was stirred for 20 min at the same temperature and allowed to warm to rt. After 10 min, Ni(II)-*meso*-purpurin-N-hexylimide **3** (100 mg, 0.13 mmol) in dry dichloromethane (15.0 mL) was added via syringe, and the resultant mixture was stirred for 36 h at rt. The reaction mixture was again cooled to 0 °C, and a saturated solution of Na_2CO_3 was added dropwise and stirred for another 8 h. The reaction mixture was then extracted with dichloromethane (3 × 50.0 mL), and the organic layers were collected, combined, and washed with water (100.0 mL). The organic layer was separated, dried over anhydrous Na_2SO_4, and concentrated. The crude product thus obtained was purified over a silica column using a 1−2% acetone/dichlormethane mixture as eluent. Yield: 80.0 mg (74.7%). UV−vis λ_{max} (in CH_2Cl_2): 690 nm (ε 3.4 × 10^4), 570 nm (ε 0.5 × 10^4), 414 nm (ε 5.7 × 10^4). ^{1}H NMR (400 MHz, $CDCl_3$): δ 9.76 (d, 1H, -CHO), 8.78 (s, 1H, *meso*-H), 8.48 (s, 1H, *meso*-H), 8.34 (d, 1H, 20^1-$\underline{CH}$, J = 15.2 Hz), 5.81 (dd, 1H, 20^2-$\underline{CH}$, J = 7.6 and 15.6 Hz), 4.55 (dd, 1H, 17-H, J = 3.6 and 8.8 Hz), 4.35 (q, 1H, 18-H, J = 6.8 Hz), 4.21 (q, 2H, N-CH_2-hexyl, J = 6.8 Hz), 3.65 (s, 3H, CO_2Me), 3.40 (s, 3H, ring-CH_3), 3.38−3.26 (m, 4H, 3-$\underline{CH_2}CH_3$ and 8-$\underline{CH_2}CH_3$), 2.88 (s, 3H, ring-CH_3), 2.70−2.65 (m, 5H, ring-CH_3, 17^2-$\underline{CH_2}$), 2.22 (m, 1H, 17^1-C$\underline{H}$H), 2.01 (m, 1H, 17^1-CH$\underline{H}$), 1.81 (m, 2H, CH_2-hexyl), 1.58−1.41 (m, 8H, 3-$CH_2\underline{CH_3}$, 8-$CH_2\underline{CH_3}$, and CH_2-hexyl), 1.39−1.34 (m, 4H, $2CH_2$-hexyl), 1.19 (d, 3H, 18-CH_3, J = 6.8 Hz), 0.93 (t, 3H, CH_3-hexyl, J = 7.2 Hz). EIMS (*m*/*z*): 797 (M^+ + Na). HRMS: calcd for $C_{43}H_{49}N_5NiO_5$ 773.3087, found 773.3076.

Benzoisobacteriopurpurin-18-N-hexylimide Methyl Ester (6) [$TiCl_3(DME)_{1.5}$ Method]. In a two-necked 100 mL dry round-bottomed flask, $TiCl_3$ (153 mg, 1 mmol) was placed, and then dry DME (5 mL) was added, and the solution was refluxed for 24 h. To this refluxing solution was added a zinc−copper alloy (176 mg, 2.5 mmol), and refluxing was continued for another 2 h. Then, Ni(II)-20-formyl-*meso*-purpurin-N-hexylimide **4** (40.0 mg, 0.052 mmol) in 10 mL of dry DME was added slowly via syringe to the reaction mixture, and the entire mixture was stirred for 45 min at the same temperature. The mixture was cooled and concentrated to dryness under vacuum. The crude product was dissolved in CH_2Cl_2 and washed with brine solution, and then the organic layer was separated, dried, and concentrated. The product was purified over a silica gel column using a 1−3% acetone/CH_2Cl_2 mixture as eluent. Yield: 12 mg (42%). UV−vis λ_{max} (in CH_2Cl_2): 687 nm. ^{1}H NMR (400 MHz, $CDCl_3$): δ 8.20 (s, 1H, *meso*-H), 8.14 (d, 1H, J = 8.4 Hz, Ph-H), 7.66 (d, 1H, J = 6.8 Hz, Ph-H), 7.52 (t, 1H, J = 8.4 Hz, Ph-H), 7.15 (s, 1H, *meso*-H), 4.50 (m, 1H), 4.11−4.21 (m, 3H), 3,54 (s, 3H, CO_2Me), 3.17 (s, 3H), 2.65 (s, 3H), 2.40−2.46 (m, 1H), 2.32 (q, 2H, J = 7.2 Hz), 1.98−2.01 (m, 1H), 1.75−1.80 (m, 3H), 1.61 (m, 3H), 1.49 (d, 3H, J = 7.2 Hz), 1.43 (t, 3H, J = 7.2 Hz), 1.38−1.39 (m, 6H), 1.26 (s, 3H), 0.89 (t, 3H, J = 13.2 Hz), 0.26 (t, 3H, J = 7.2 Hz). EIMS (*m*/*z*): 781 (M + Na). HRMS: calcd for $C_{43}H_{49}N_5NiO_4$ 757.3138, found 757.3120.

Ni-3-(Vinyl)-bistrifluoromethylbenzyl-purpurinimide (8). 3-(Vinyl)-bistrifluromethylbenzyl-purpurinimide (200.0 mg, 0.25 mmol) was dissolved in 50 mL of toluene, and nickel acetylacetonate hydrate (640.0 mg, 2.45 mmol) was added to it. The reaction mixture was refluxed vigorously for 2 h, and progress of the reaction was monitored by TLC and UV−vis. After completion, the reaction mixture was cooled and directly loaded onto a silica column. Product **8** was eluted with a 1% acetone/dichloromethane mixture. Yield: 195.0 mg (91.1%). UV−vis λ_{max} (in CH_2Cl_2): 675 nm (ε 4.1 × 10^4), 548 nm (ε 0.5 × 10^4), 423 nm (ε 6.9 × 10^4), 379 nm (ε 3.9 × 10^4). ^{1}H NMR (400 MHz, $CDCl_3$): δ 9.00 (s, 1H, *meso*-H), 8.73 (s, 1H, *meso*-H), 8.09 (s, 2H, Ph-H), 7.91 (s, 1H, *meso*-H), 7.78 (s, 1H, Ph-H), 7.55 (dd, 1H, -$\underline{CH}$=CH_2, J = 11.6 and 17.6 Hz), 5.93 (d, 1H, -CH=C$\underline{H_2}$, J = 10.4 Hz), 5.91 (d, 1H, -CH=C$\underline{H_2}$, J = 4.0 Hz), 5.59 (s, 2H, N-$\underline{CH_2}$-Ph), 4.72 (m, 1H, 17-H), 4.06 (q, 1H, 18-H, J = 7.2 Hz), 3.60 (s, 3H, CO_2Me), 3.49 (s, 3H, ring-CH_3), 3.40 (m, 2H, 8-$\underline{CH_2}CH_3$), 2.98 (s, 3H, ring-CH_3), 2.93 (s, 3H, ring-CH_3), 2.63−2.56 (m, 2H, 17^2-CH_2), 2.19 (m, 1H, 17^1-CH_2), 1.92 (m, 1H, 17^1-CH_2), 1.50 (t, 3H, 8-$CH_2\underline{CH_3}$, J = 7.2 Hz), 1.32 (d, 3H, 18-CH_3, J = 6.8 Hz). EIMS (*m*/*z*): 861 (M + H). HRMS: calcd for $C_{43}H_{37}F_6N_5NiO_4$ 859.2103, found 859.2107.

***meso*-Ni-Bistrifluoromethylbenzyl-purpurinimide (9).** Ni-3-(Vinyl)-bistrifluoromethylbenzyl-purpurinimide (300.0 mg, 0.34 mmol) was dissolved in 100 mL of distilled THF. Pd/C (10% w/w, 600.0 mg) and 5 or 6 drops of triethylamine were added to the reaction mixture. The reaction mixture was flushed with H_2 and stirred vigorously for 12 h under H_2 atmosphere. Progress of the reaction was monitored by UV−vis and ^{1}H NMR. After completion, the reaction mixture was degassed, flushed with N_2, and filtered over a Celite bed. The filtrate was concentrated, and the crude product was purified over an alumina (G-III) column using a 0.5−1% acetone/dichloromethane mixture as eluent. Yield: 280.0 mg (93.1%). UV−vis λ_{max} (in CH_2Cl_2): 664 nm (ε 3.2 × 10^4), 545 nm (ε 0.4 × 10^4), 420 nm (ε 6.0 × 10^4). ^{1}H NMR (400 MHz, $CDCl_3$): δ 8.98 (s, 1H, *meso*-H), 8.59 (s, 1H, *meso*-H), 8.08 (s, 2H, Ph-H), 7.85 (s, 1H, *meso*-H), 7.77 (s, 1H, Ph-H), 5.58 (s, 2H, N-$\underline{CH_2}$-Ph), 4.71 (dd, 1H, 17-H, J = 3.60 and 8.80 Hz), 4.04 (q, 1H, 18-H, J = 7.2 Hz), 3.58 (s, 3H, CO_2Me), 3.46 (s, 3H, ring-CH_3), 3.42−3.34 (m, 4H, 3-$\underline{CH_2}CH_3$ and 8-$\underline{CH_2}CH_3$), 2.94 (s, 3H, ring-CH_3), 2.86 (s, 3H, ring-CH_3), 2.62−2.55 (m, 2H, 17^2-CH_2), 2.16−2.13 (m, 1H, 17^1-CH_2), 1.93−1.89 (m, 1H, 17^1-CH_2), 1.55−1.48 (m, 7H, 3-$CH_2\underline{CH_3}$ and 8-$CH_2\underline{CH_3}$), 1.32 (d, 3H, 18-

CH_3, $J = 6.8$ Hz). EIMS (*m*/*z*): 863 (M + H). HRMS: calcd for $C_{43}H_{39}F_6N_5NiO_4$ 861.2260, found 861.2263.

Benzoisobacteriopurpurin-18-N-(3,5-trifluoromethylbenzyl)-imide Methyl Ester (11) [$TiCl_3(DME)_{1.5}$ Method]. Yield: 29 mg (36%). UV−vis λ_{max} (in CH_2Cl_2): 609 nm. ^{1}H NMR (400 MHz, $CDCl_3$): δ 8.78 (s, 1H, *meso*-H), 8.46 (s, 1H, *meso*-H), 8.31 (d, 1H, 20^1-CH, $J = 15.2$ Hz), 8.03 (s, 2H, Ph-H), 7.77 (s, 1H, Ph-H), 5.80 (dd, 1H, 20^2-CH, $J = 7.6$ and 15.6 Hz), 5.52 (s, 2H, benzylic-CH_2), 4.49 (dd, 1H, 17-H, $J = 4.0$ and 8.8 Hz), 4.32 (q, 1H, 18-H, $J = 7.2$ Hz), 3.63 (s, 3H, CO_2Me), 3.38 (s, 3H, ring-CH_3), 3.35−3.27 (m, 4H, 3-$\underline{CH_2}CH_3$ and 8-$\underline{CH_2}CH_3$), 2.87 (s, 3H, ring-CH_3), 2.66 (s, 3H, ring-CH_3), 2.64−2.61 (m, 2H, 17^2-CH_2), 2.18 (m, 2H, 17^1-CH_2), 2.00 (m, 1H, 17^1-CH_2), 1.47 (t, 3H, 8-$CH_2\underline{CH_3}$, $J = 7.2$ Hz), 1.46 (t, 3H, 3-$CH_2\underline{CH_3}$, $J = 7.2$ Hz), 1.16 (d, 3H, 18-CH_3, $J = 6.8$ Hz). EIMS (*m*/*z*): 921 (M + Na). HRMS: calcd for $C_{46}H_{41}F_6N_5NiO_4$ 899.2416, found 899.2408.

Dihydrobenzoisobacteriopurpurin-18-N-(3,5-trifluoromethylbenzyl)imide Methyl Ester (12) [$TiCl_3(DME)_{1.5}$ Method]. Yield: 35 mg (44%). UV−vis λ_{max} (in CH_2Cl_2) 663 nm. ^{1}H NMR (400 MHz, $CDCl_3$): δ 8.26 (s, 1H, *meso*-H), 8.00 (s, 2H, Ph-H), 7.74 (s, 1H, *meso*-H), 7.20 (s, 1H, Ph-H), 6.82 (dd, 1H, 20^1-CH, $J = 3.2$ and 9.6 Hz), 6.08 (m, 1H, 20^1-CH), 5.47 (s, 2H, benzylic-CH_2), 4.63 (dd, 1H, 17-H, $J = 3.6$ and 8.4 Hz), 3.56 (q, 1H, 18-H, $J = 6.8$ Hz), 3.55 (s, 3H, CO_2Me), 3.15 (s, 3H, ring-CH_3), 3.13−3.11 (m, 3H, 8-$\underline{CH_2}CH_3$ and 3-CH), 2.85− 2.82 (dd, 1H, 20^3-C$\underline{H}$H, $J = 6.4$ and 16.4 Hz), 2.63−2.60 (dd, 1H, 20^3-CH$\underline{H}$, $J = 6.4$ and 16.4 Hz), 2.58 (s, 3H, ring-CH_3), 2.42−2.35 (m, 2H, 3-C$\underline{H}$HCH$_3$ and 17^2-C$\underline{H}$H), 2.27 (m, 1H, 17^2-CH$\underline{H}$), 2.10 (m, 1H, 3-CH$\underline{H}$CH$_3$), 2.07 (m, 1H, 17^1-C$\underline{H}$H), 1.85 (m, 1H, 17^1-CH$\underline{H}$), 1.82 (s, 3H, 2-CH_3), 1.39 (t, 3H, 8-$CH_2\underline{CH_3}$, $J = 7.6$ Hz), 1.35 (t, 3H, 3-$CH_2\underline{CH_3}$, $J = 7.2$ Hz), 1.28 (d, 3H, 18-CH_3, $J = 7.2$ Hz). EIMS (*m*/*z*): 923 (M + Na). HRMS: calcd for $C_{46}H_{43}F_6N_5NiO_4$ 901.2573, found 901.2565.

1,2-Bis[Ni(II)-*meso*-purpurin-18-N-hexylimide]ethane (13). In a two-necked 100 mL dry round-bottomed flask, dry THF (15 mL) and zinc metal (16.78 mg, 0.25 mmol) were placed and refluxed under N_2 atmosphere. To this refluxing solution was added dropwise $TiCl_4$ (1 M solution in toluene, 0.128 mL, 0.128 mmol), and the resulting mixture was stirred for 2 h under reflux. After 2 h, Ni(II)-20-formyl-*meso*-purpurin-N-hexylimide **4** (48.0 mg, 0.064 mmol) in 10 mL of dry THF was added slowly via a syringe, and the reaction mixture was further stirred for 45 min at the same temperature. The mixture was then cooled and concentrated to dryness under vacuum. The crude product was dissolved in CH_2Cl_2 and washed with a brine solution, and then the organic layer was separated, dried, and concentrated. The product was purified over a silica gel column using a 1−3% acetone/dichloromethane mixture as eluent. Yield: 20.0 mg (42.5%). UV−vis λ_{max} (in CH_2Cl_2): 687 nm (ε 5.3×10^4), 426 nm (ε 9.4×10^4). ^{1}H NMR (400 MHz, $CDCl_3$): δ 8.85 (s, 1H, *meso*-H), 8.55 (s, 1H, *meso*-H), 7.09 (s, 1H, 20^1-CH), 4.53 (dd, 1H, 17-H, $J = 3.6$ and 8.8 Hz), 4.32 (q, 1H, 18-H, $J = 7.2$ Hz), 4.21 (q, 2H, N-CH_2-hexyl, $J = 6.8$ Hz), 3.62 (s, 3H, CO_2Me), 3.43 (s, 3H, ring-CH_3), 3.41−3.33 (m, 4H, 3-$\underline{CH_2}CH_3$ and 8-$\underline{CH_2}CH_3$), 2.94 (s, 3H, ring-CH_3), 2.71 (s, 3H, ring-CH_3), 2.69−2.63 (m, 2H, 172-CH_2), 2.24 (m, 1H, 17^1-C$\underline{H}$H), 2.06 (m, 1H, 17^1-CH$\underline{H}$), 1.81 (m, 2H, CH_2-hexyl), 1.52−1.43 (m, 8H, 3-$CH_2\underline{CH_3}$, 8-$CH_2\underline{CH_3}$, and CH_2-hexyl), 1.39−1.31 (m, 4H, 2CH_2-hexyl), 1.09 (d, 3H, 18-CH_3, $J = 6.8$ Hz), 0.90 (t, 3H, CH_3-hexyl, $J = 7.2$ Hz). ^{13}C NMR (100 MHz, $CDCl_3$): δ 173.9, 166.5, 162.8, 160.3, 156.7, 149.6, 148.9, 146.1, 143.5, 143.3, 141.1, 139.1, 139.0, 136.1, 135.9, 133.6, 133.3, 120.6, 109.0, 108.2, 104.7, 97.6, 54.3, 51.6, 46.8, 39.8, 32.3, 31.7, 29.7, 28.8, 27.3, 27.0, 22.7, 19.5, 19.0, 17.0, 16.6, 15.7, 14.1, 12.2, 10.5. EIMS (*m*/*z*): positive mode, 1488 (M^+ + Na); negative mode, 1464 (M^- − H). HRMS: calcd for $C_{82}H_{94}N_{10}Ni_2O_8$ 1462.5963, found 1462.5953.

***trans-trans-trans*-1,6-Bis[Ni(II)-*meso*-purpurin-18-N-hexylimide methyl ester-1,3,5-hexatriene] (15).** In a two-necked 100 mL dry round-bottomed flask, dry THF (15 mL) and zinc metal (16.78 mg, 0.25 mmol) were placed and refluxed under N_2 atmosphere. To this refluxing solution was added dropwise $TiCl_4$ (1 M solution in toluene, 0.129 mL, 0.129 mmol), and the resultant mixture was stirred for 2 h under reflux. After 2 h, Ni(II)-20-vinylformyl-*meso*-purpurin-N-hexylimide **5** (50.0 mg, 0.064 mmol) in 10 mL of dry THF was added slowly via a syringe, and the reaction mixture was further stirred for 45 min at the same temperature. The reaction mixture was cooled and concentrated to dryness under vacuum. The crude sample was dissolved in dichloromethane and washed with brine solution, and then the organic layer was separated, dried, and concentrated. The product was purified over a silica gel column using a 1−3% acetone/CH_2Cl_2 mixture as an eluent. Yield: 15.0 mg (30.6%). UV−vis λ_{max} (in CH_2Cl_2): 696 nm (ε 5.8×10^4), 430 nm (ε 11.3×10^4). ^{1}H NMR (400 MHz, $CDCl_3$): δ 8.86 (s, 1H, *meso*-H), 8.56 (s, 1H, *meso*-H), 7.44 (d, 1H, 20^1-$\underline{CH}$, $J = 15.2$ Hz), 6.45 (dd, 1H, 20^2-$\underline{CH}$, $J = 2.8$ and 6.8 Hz), 5.72 (ddd, 1H, 20^3-$\underline{CH}$, $J = 2.8$ and 6.8 Hz), 4.50 (dd, 1H, 17-H, $J = 3.8$ and 9.2 Hz), 4.19 (m, 3H, 18-H and N-$\underline{CH_2}$-hexyl), 3.61 (s, 3H, $CO_2\underline{Me}$), 3.42 (s, 3H, ring-CH_3), 3.40−3.35 (m, 4H, 3-$\underline{CH_2}CH_3$ and 8-$\underline{CH_2}CH_3$), 2.96 (s, 3H, ring-CH_3), 2.79 (s, 3H, ring-CH_3), 2.61 (t, 2H, 172-$\underline{CH_2}$, $J = 8.0$ Hz), 2.20 (m, 1H, 17^1-C$\underline{H}$H), 1.98 (m, 1H, 17^1-CH$\underline{H}$), 1.81 (m, 2H, $\underline{CH_2}$-hexyl), 1.56−1.41 (m, 8H, 3-$CH_2\underline{CH_3}$, 8-$CH_2\underline{CH_3}$ and CH_2-hexyl), 1.39−1.33 (m, 4H, 2$\underline{CH_2}$-hexyl), 1.03 (d, 3H, 18-CH_3, $J = 6.8$ Hz), 0.88 (t, 3H, $\underline{CH_3}$-hexyl, $J = 6.8$ Hz). ^{13}C NMR (100 MHz, $CDCl_3$): δ 173.9, 166.5, 162.8, 160.2, 157.6, 149.5, 149.4, 145.3, 143.6, 143.5, 142.2, 140.8, 139.1, 138.7, 135.8, 134.7, 133.8, 133.1, 129.3, 120.3, 108.8, 107.1, 103.6, 97.8, 53.4, 51.5, 46.7, 39.8, 32.2, 31.7, 29.7, 28.8, 28.0, 27.0, 22.7, 19.0, 18.8, 17.0, 16.7, 16.0, 14.0, 12.2, 10.5. EIMS (*m*/*z*): positive mode, 1540 (M^+ + Na); negative mode, 1516 (M^- − H). HRMS: calcd for $C_{86}H_{98}N_{10}Ni_2O_8$ 1514.6276, found 1514.6297.

Ni(II)-3-Formyl-3-devinyl-purpurin-18-N-hexylimide Methyl Ester (16). To a solution of Ni-purpurin-18-N-hexylimide methyl ester **2** (300 mg, 0.42 mmol) in THF (80 mL) were added a solution of OsO_4 (118 mg, 0.46 mmol) in CCl_4 (20 mL) and a solution of $NaIO_4$ (1.8 g, 8.4 mmol) in water (50 mL), successively. The mixture was stirred at rt for 6 h, diluted with CH_2Cl_2 (300 mL), washed with water, and dried with Na_2SO_4. The solvent was removed, and the residue was purified with column chromatography on alumina, eluting with a 0.5% acetone/CH_2Cl_2 (v/v 40/1) mixture to provide the compound as dark brown plates. Yield: 190 mg 63%). UV−vis λ_{max} (in CH_2Cl_2): 708 nm (ε 5.3×10^4), 565 nm (ε 0.6×10^4), 433 nm (ε 6.3×10^4), 388 nm (ε 4.2×10^4). ^{1}H NMR (400 MHz, $CDCl_3$): δ 10.95 (s, 1H, -CHO), 9.69 (s, 1H, *meso*-H), 9.10 (s, 1H, *meso*-H), 8.10 (s, 1H, *meso*-H), 4.82 (d, 1H, 17-H, $J = 9.2$ Hz), 4.29 (m, 2H, N-$\underline{CH_2}$-hexyl), 4.13 (q, 1H, 18-H, $J = 7.2$ Hz), 3.62 (s, 3H, CO_2Me), 3.54 (s, 3H, ring-CH_3), 3.46 (m, 2H, 8-$\underline{CH_2}CH_3$), 3.33 (s, 3H, ring-CH_3), 3.03 (s, 3H, ring-CH_3), 2.66 (m, 1H, 17^2-C$\underline{H}$H), 2.58 (m, 1H, 17^2-CH$\underline{H}$), 2.21 (m, 1H, 17^1-CHH), 1.94 (m, 1H, 17^1-CH$\underline{H}$), 1.87 (m, 2H, -CH_2-hexyl), 1.56 (t, 3H, 8-$CH_2\underline{CH_3}$, $J = 7.6$ Hz), 1.52 (m, 2H, -CH_2-hexyl), 1.41 (m, 4H, −2CH_2-hexyl), 1.35 (d, 3H, 18-CH_3, $J = 6.8$ Hz), 0.93 (t, 3H, CH_3-hexyl, $J = 6.8$ Hz). EIMS (*m*/*z*): 743 (M^+ + Na). HRMS: calcd for $C_{39}H_{43}N_5NiO_5$ 719.2618, found 719.2610.

Ni(II)-3-(2-Formylvinyl)-3-devinyl-purpurin-18-N-hexylimide Methyl Ester (17). In a two-necked 100 mL dry round-bottomed flask, a mixture of N,N-dimethyformamide (1.0 mL) and dry dichloromethane (20.0 mL) was cooled to 0 °C under N_2 atmosphere. To this cooled mixture was added $POCl_3$ (1.0 mL) slowly via syringe under continuous stirring. The reaction mixture was stirred for 20 min at the same temperature and then allowed to warm to rt. After 10 min, Ni(II)-3-vinyl-purpurin-N-hexylimide **2** (100.0 mg, 0.13 mmol) in dry dichloromethane (15.0 mL) was added via syringe, and the resultant mixture was stirred for 36 h at rt. The reaction mixture was again cooled to 0 °C, and a saturated solution of Na_2CO_3 was added dropwise. The resultant mixture was stirred for another 8 h. The reaction mixture was then extracted with dichloromethane (3 × 50.0 mL), and the organic layer was collected, combined, and washed with water (100 mL). It was then separated, dried over anhydrous Na_2SO_4, and concentrated. The crude product thus obtained was purified over a silica column using

a 1−2% acetone/dichlormethane mixture as eluent. Yield: 70.0 mg (67.9%). UV−vis λ_{max} (in CH_2Cl_2): 704 nm (ε 4.8 × 10^4), 561 nm (ε 0.6 × 10^4), 427 nm (ε 5.2 × 10^4), 394 nm (ε 4.6 × 10^4), 330 nm (ε 2.9 × 10^4). ^{1}H NMR (400 MHz, $CDCl_3$): δ 9.96 (d 1H, -CHO, J = 7.2 Hz), 9.04 (s, 1H, *meso*-H), 8.74 (s, 1H, *meso*-H), 8.31 (dd, 1H, 3-CH=CH-CHO, J = 16.0 Hz), 8.03 (s, 1H, *meso*-H), 6.96 (dd, 1H, 3-CH=CH-CHO, J = 7.6 and 16.0 Hz), 4.78 (dd, 1H, 17-H, J = 2.8 and 9.2 Hz), 4.28 (m, 2H, N-CH_2-hexyl), 4.12 (q, 1H, 18-H, J = 6.8 Hz), 3.64 (s, 3H, CO_2Me), 3.51 (s, 3H, ring-CH_3), 3.47−3.38 (m, 2H, 8-CH_2CH_3), 3.09 (s, 3H, ring-CH_3), 2.96 (s, 3H, ring-CH_3), 2.71−2.68 (m, 1H, 17^2-CHH), 2.63−2.60 (m, 1H, 17^2-CHH), 2.25−2.23 (m, 1H, 17^1-CHH), 1.94−1.90 (m, 1H, 17^1-CHH), 1.88−1.85 (m, 2H, CH_2-hexyl), 1.55−1.49 (m, 5H, 8-CH_2CH_3 and -CH_2-hexyl), 1.45−1.37 (m, 4H, 2CH_2-hexyl), 1.34 (d, 3H, 18-CH_3, J = 6.8 Hz), 0.93 (t, 3H, CH_3-hexyl, J = 6.8 Hz). EIMS (*m*/*z*): 769 (M^+ + Na). HRMS: calcd for $C_{41}H_{45}N_5NiO_5$ 745.2774, found 745.2764.

Bis-3-[Ni(II)-purpurin-18-N-hexylimide]ethane (18). In a two-necked dry 100 mL round-bottomed flask, dry THF (15 mL) and zinc metal (18.16 mg, 0.27 mmol) were placed and refluxed under N_2 atmosphere. To this refluxing solution was added dropwise $TiCl_4$ (1 M solution in toluene, 0.138 mL, 0.138 mmol), and the resultant mixture was stirred for 2 h under refluxing. After 2 h, Ni(II)-3-formyl-3-devinyl-purpurin-N-hexylimide **16** (50.0 mg, 0.069 mmol) in 10 mL of dry THF was added slowly via syringe, and the reaction mixture was further stirred for 45 min at the same temperature. It was then cooled and concentrated to dryness under vacuum. The crude product was dissolved in dichloromethane and washed with brine solution, and the organic layer was separated, dried, concentrated, and purified over a silica gel column using a 1−3% acetone/dichloromethane mixture as eluent. Yield: 16.0 mg (32.7%). UV−vis λ_{max} (in CH_2Cl_2): 708 nm (ε 6.3 × 10^4), 557 nm (ε 1.1 × 10^4), 422 nm (ε 11.4 × 10^4). ^{1}H NMR (400 MHz, $CDCl_3$): δ 9.08 (s, 1H, *meso*-H), 9.06 (s, 1H, *meso*-H), 8.15 (s, 1H, *meso*-H), 8.06 (s, 1H, 3^1-CH), 4.83 (dd, 1H, 17-H, J = 2.8 and 8.8 Hz), 4.30 (m, 2H, N-CH_2-hexyl), 4.16 (q, 1H, 18-H, J = 7.2 Hz), 3.65 (s, 3H, CO_2Me), 3.53 (s, 3H, ring-CH_3), 3.45 (m, 2H, 8-CH_2CH_3), 3.27 (s, 3H, ring-CH_3), 2.94 (s, 3H, ring-CH_3), 2.70 (m, 1H, 17^2-CHH), 2.62 (m, 1H, 17^2-CHH), 2.29 (m, 1H, 17^1-CHH), 2.02 (m, 1H, 17^1-CHH), 1.88 (m, 2H, -CH_2-hexyl), 1.52 (m, 5H, 8-CH_2CH_3, -CH_2-hexyl), 1.46−1.38 (m, 7H, -2CH_2-hexyl and 18-CH_3), 0.93 (t, 3H, CH_3-hexyl, J = 6.8 Hz). ^{13}C NMR (100 MHz, $CDCl_3$): δ 173.8, 166.7, 162.8, 162.5, 160.0, 149.4, 145.8, 143.6, 143.5, 141.9, 141.3, 139.6, 139.0, 136.1, 134.1, 133.7, 127.6, 120.4, 108.4, 104.6, 97.8, 95.0, 51.6, 47.6, 40.0, 32.1, 31.7, 29.7, 28.8, 28.7, 27.1, 22.7, 20.9, 19.1, 17.1, 14.1, 12.3, 12.2, 10.8. EIMS (*m*/*z*): 1431 (M^+ + Na). HRMS: calcd for $C_{78}H_{86}N_{10}Ni_2O_8$ 1406.5337, found 1406.5325.

***trans-trans-trans*-1,6-Bis[3-Ni(II)-purpurin-18-N-hexylimide methyl ester] (19).** In a two-necked 100 mL dry round-bottomed flask, dry THF (15 mL) and zinc metal (17.5 mg, 0.26 mmol) were refluxed under N_2 atmosphere. To this refluxing solution was added dropwise $TiCl_4$ (1 M solution in toluene, 0.134 mL, 0.134 mmol), and the resultant mixture was stirred for 2 h under reflux. After 2 h, Ni-20-vinylformyl-*meso*-purpurin-N-hexylimide **17** (50.0 mg, 0.067 mmol) in 10 mL of dry THF was added slowly via a syringe, and the reaction mixture was further stirred for 30−45 min at the same temperature. The reaction mixture was cooled and concentrated to dryness under vacuum. The crude product was dissolved in dichloromethane and washed with brine solution, and the organic layer was separated, dried, and concentrated. It was purified over a silica gel column using a 1−3% acetone/CH_2Cl_2 mixture as eluent. Yield: 15.0 mg (30.6%). UV−vis λ_{max} (in CH_2Cl_2): 715 nm (ε 6.1 × 10^4), 560 nm (ε 1.5 × 10^4), 422 nm (ε 10.3 × 10^4). ^{1}H NMR (400 MHz, $CDCl_3$): δ 9.03 (s, 1H, *meso*-H), 8.83 (s, 1H, *meso*-H), 7.95 (s, 1H, *meso*-H), 7.64 (d, 1H, 3^1-CH, J = 15.2 Hz), 7.29 (m, 1H, 3^2-CH), 7.05 (dd, 1H, 3^3-CH, J = 3.2 and 7.2 Hz), 4.79 (dd, 1H, 17-H, J = 2.3 and 8.8 Hz), 4.28 (m, 2H, N-CH_2-hexyl), 4.10 (q, 1H, 18-H, J = 6.8 Hz), 3.63 (s, 3H, CO_2Me), 3.51 (s, 3H, ring-CH_3), 3.48−3.39 (m, 2H, 8-CH_2CH_3), 3.11 (s, 3H, ring-CH_3), 2.99 (s, 3H, ring-CH_3), 2.67 (m, 1H, 17^2-CHH), 2.60 (m, 1H, 17^2-CHH), 2.25 (m, 1H, 17^1-CHH), 1.99 (m, 1H, 17^1-CHH), 1.89−1.83 (m, 2H, CH_2-hexyl), 1.54−1.51 (m, 5H, 8-CH_2CH_3 and CH_2-hexyl), 1.48−1.41 (m, 4H, 2CH_2-hexyl), 1.35 (d, 3H, 18-CH_3, J = 6.8 Hz), 0.92 (t, 3H, CH_3-hexyl, J = 6.8 Hz). ^{13}C NMR (100 MHz, $CDCl_3$): δ 173.8, 166.7, 162.8, 162.5, 160.0, 149.6, 145.6, 143.5, 142.0, 140.7, 139.8, 135.6, 135.5, 134.0, 133.2, 125.1, 121.0, 108.3, 105.0, 94.9, 51.5, 47.5, 43.9, 39.9, 32.1, 31.7, 29.7, 29.5, 29.3, 28.8, 28.7, 27.1, 22.7, 20.9, 19.1, 17.1, 16.8, 14.1, 12.3, 12.3, 10.8. HRMS: calcd for $C_{82}H_{90}N_{10}Ni_2O_8$ 1458.5650, found 1458.5641.

Electrochemical and Spectroelectrochemical Measurements. Cyclic voltammetry (CV) measurements were performed at 298 K on an EG&G model 173 potentiostat coupled with an EG&G model 175 universal programmer in deaerated benzonitrile (PhCN) solution containing 0.1 M tetra-*n*-butylammonium perchlorate (TBAP) as the supporting electrolyte. A three-electrode system was utilized and consisted of a glassy carbon working electrode, a platinum wire counter electrode, and a saturated calomel reference electrode (SCE). The reference electrode was separated from the bulk of the solution by a fritted-glass bridge filled with the solvent/supporting electrolyte mixture. Thin-layer spectroelectrochemical measurements were carried out using an optically transparent platinum thin-layer working electrode and a Hewlett-Packard model 8453 diode array spectrophotometer coupled with an EG&G model 173 universal programmer.

Molecular Modeling Computational Method. The three-dimensional structures of monomer units **4** and **16** were modeled from the crystal structure of anhydro-*meso*-rhodoisobacteriochlorin methyl ester-Ni(II)[31] as a template. Appropriate modifications, including changes of atoms and bond types and deletions and additions of atoms and bonds, were performed with the SYBYL molecular modeling program version 8.0 (Tripos, Inc.) using standard geometry. An extended conformation was assumed for the *n*-hexyl tail. The dimers **13**, **14**, and **15** were modeled from monomer unit **4** with assumed linker conformations as in Scheme 2. Similarly, the dimers **18**, **19**, and **19a** were modeled from monomer unit **16** as in Scheme 3. The geometry of each compound was first optimized with a molecular mechanics method using a Merck molecular force field (MMFF), which was followed by full optimization with a semiempirical molecular orbital method, PM3, both with Spartan software (Wavefunction, Inc.). The default parameters were used, except for the mmok option with PM3 optimization.

Acknowledgment. Financial support from the NIH (CA55791, CA127369), the Roswell Park Alliance Foundation, and the Robert A. Welch Foundation (K.M.K., Grant E-680) is gratefully acknowledged. Mass spectrometry analyses were performed at the Biopolymer Facility, Roswell Park Cancer Institute and Michigan State University, East Lansing, MI. Dr. M. P. Dobhal is thankful to Dr. N. K. Jain, Vice -Chancellor, University of Rajasthan, Jaipur, India for the study leave award.

Supporting Information Available: NMR spectra of compounds **4**−**6**, **10**−**13**, **15**−**19** and UV−vis spectra of compounds **13**, **15**, **18,** and **19**. This material is available free of charge via the Internet at http://pubs.acs.org.

JO8019237

(31) Renner, M. W.; Furenlid, L. R.; Barkigia, K. M.; Forman, A.; Shim, H.-K.; Simpson, D. J.; Smith, K. M.; Fajer, J. *J. Am. Chem. Soc.* **1991**, *113*, 6891.